# Aerodynamic Noise Prediction of Subsonic Rotors

*Jeong-Han Lee, and *Soo-Gab Lee

Abstract

Numerical predictions of aerodynamic noise radiated by subsonic rotors are carried out. A computer program has been developed which incorporates both the discrete frequency noise as well as the broadband noise arising from the ingestion of turbulence. Acoustic analogy is used in conjunction with Homicz's formulation of turbulence ingestion noise. Formulation 1A of Farassat is used to enhance the numerical analysis performance of Ffowcs-Williams Hawkings equation by eliminating the numerical time differentiation. Homicz's turbulence ingestion noise prediction technique is used to understand the characteristics of broadband noise radiated by isotropic turbulence ingestion.

Numerical predictions are carried out for a number of rotor configurations and compared with experimental data. Monopole consideration of transonic rotor agrees well with both the experimental data and the linear theory. Noise radiation characteristics of rotor at lifting hover are investigated utilizing simple blade loading obtained by thin wing section theory. By incorporating discrete noise prediction of steady loading with broadband spectrum, much better agreement with experimental data is obtained in the low frequency region. The contributions from different noise mechanisms can also be analyzed through this method.

## Ⅰ. Introduction

In various industrial applications, the aerodynamic noise radiated by rotors are receiving increased attention as the regulations are becoming severer. The strong demand for quiet products from the customers also strengthen the need to limit noise emissions from rotors or fans, previously considered only secondary to the total noise radiated by the whole system. Over the past several years, noise levels from primary sources such as the propulsion devices have been successfully reduced. The acoustic consideration of secondary sources such as rotors or fans have thus become imperative in satisfying the new regulations and the need for environment-friendly products.

Due to a large amount of research carried out involving the helicopter rotor noise predictions, impulsive noise from high speed rotors are understood to a reasonable degree.[1] The main goal of this study is to apply the rotor noise prediction techniques to low speed rotors and to investigate the noise prediction capabilities. The aeroacoustic investigation of low speed rotors prelude those of fans and blowers used in diverse industrial sectors. Previous development of fan and blower designs involved experimental evaluation of noise which required significant experimental activity. Low speed rotor noise prediction tools could be extended to enhance the designing process of low noise commercial fans. This type of transfer of aerospace technology to commercial products is underway in many areas.[2]

The noise radiated by rotors can be classified as either discrete frequency or broadband noise depending on the type of spectrum they exhibit. Steady and periodic blade loads incur discrete frequency noise while a number of unsteady and random disturbances such as turbulence ingestion, turbulent boundary layer/trailing edge interaction, and 3-D unsteady tip flow are the sources for broadband noise. In this study, monopole and dipole terms from the Ffowcs-Williams Hawkings equation[3] of acoustic analogy[4] are evaluated as the discrete frequency noise sources while turbulence ingestion noise is considered as the fundamental broadband noise source.

## Ⅱ. Discrete Frequency Noise

Ffowcs Williams and Hawkings have formulated the following equation for the manifestation of acoustic analogy first proposed by Lighthill.

$$\frac{1}{c_0^2}\frac{\partial^2 p'}{\partial t^2}-\nabla^2 p'=\frac{\partial}{\partial t}\left[\rho_0 v_n|\nabla f|\delta(f)\right] \qquad (1)$$
$$-\frac{\partial}{\partial x_i}\left[l_i|\nabla f|\delta(f)\right]-\frac{\partial^2}{\partial x_i\partial x_j}\left[T_{ij}H(f)\right]$$

*Department of Aerospace Engineering, Seoul National University

Manuscript Received: March 14, 1997.

The equation is composed of three terms each corresponding to the monopole, dipole, and quadrupole source contributions. $\rho_0$ and $c_0$ are the density and speed of sound in the undisturbed medium while the acoustic pressure is written as $p'$. $l_i$ is the force per unit area exerted on the fluid by the solid surface and $v_n$ is the surface normal velocity. The Lighthill stress tensor, $T_{ij}$ is neglected in this study since only low speed rotors are considered. The $\delta(f)$ and $H(f)$ denote Dirac delta function and Heaviside function, respectively.

Through the use of Green's function and coordinate transformations, the solution for the acoustic pressure was obtained by Farassat in the following form.[5]

$$4\pi p'(\vec{x},t)=\frac{1}{c_0}\frac{\partial}{\partial t}\int_{f=0}\left[\frac{\rho_0 c_0 v_n+l_r}{r|1-M_r|}\right]_{ret}dS+\int_{f=0}\left[\frac{l_r}{r^2|1-M_r|}\right]_{ret}dS$$

The integrals taken on the $f=0$ denote that the integral be taken on the body surface, while the subscript $ret$ denotes that the integrands be evaluated at the retarded time. The difficulties introduced when numerically evaluating the above equation is overcome by using the following relations.

$$\frac{\partial r}{\partial \tau}=-v_r,\quad \frac{\partial \hat{r}_i}{\partial \tau}=\frac{\hat{r}_i v_r-v_i}{r},\quad \frac{\partial M_r}{\partial \tau}=\frac{1}{c_0 r}\left(r_i\frac{\partial v_i}{\partial \tau}+v_r^2-v^2\right),$$

$$\frac{\partial v_n}{\partial \tau}=\left(\frac{\partial v_i}{\partial \tau}\hat{n}_i+v_i\frac{\partial \hat{n}_i}{\partial \tau}\right)\equiv \dot{v}_n$$

Using the above, Farassat's 1A formulation is written in the following form.[6]

$$p'(\vec{x},t)=p'_T(\vec{x},t)+p'_l(\vec{x},t) \tag{2}$$

$$4\pi p'_T(\vec{x},t)=\int_{f=0}\left[\frac{\rho_0\dot{v}_n}{r(1-M_r)^2}\right]_{ret}dS+\int_{f=0}\left[\frac{\rho_0 v_n\left(r\dot{M}_i\hat{r}_i+c_0M_r-c_0M^2\right)}{r^2(1-M_r)^3}\right]_{ret}dS \tag{2.1}$$

$$4\pi p'_l(\vec{x},t)=\frac{1}{c_0}\int_{f=0}\left[\frac{\dot{l}_i\hat{r}_i}{r(1-M_r)^2}\right]_{ret}dS+\int_{f=0}\left[\frac{l_r-l_iM_i}{r^2(1-M_r)^2}\right]_{ret}dS+\frac{1}{c_0}\int_{f=0}\left[\frac{l_r\left(r\dot{M}_i\hat{r}_i+c_0M_r-c_0M^2\right)}{r^2(1-M_r)^3}\right]_{ret}dS \tag{2.2}$$

Formulation 1A eliminates the numerical time differentiation procedure and is valid for arbitrary blade motion and geometry. The near-field terms and the far-field terms are seen explicitly with $\frac{1}{r^2}$ and $\frac{1}{r}$, respectively. $p'_T(\vec{x},t)$ and $p'_l(\vec{x},t)$ represent thickness and loading terms, respectively, and correspond to the monopole and dipole terms in equation (1). The dots in $\dot{M}_i$ and $\dot{l}_i$ denote time differentiation with respect to the retarded time, and the subscript $r$ denote the direction towards the observer.

A computer program has been developed taking full advantage of the formulation. The program is able to handle blade geometry of arbitrary shape and motion. The calculations are performed on the surface of the blade which is divided into a number of panels used for integration. Since the acoustic calculations are performed in the ground fixed frame, a series of coordinate transformations are necessary. Any form of blade loading can be used as input. Unsteady loading, or even impulsive loading can be used as input, as long as the data is of reasonable resolution, both in spatial and sequential terms.

## Ⅲ. Broadband Noise

Of the broadband noise mechanisms related to all random aerodynamic processes which can occur, turbulence ingestion noise is believed to cover the range of practical applications. Homicz[7] derived an exact solution appropriate to the noise due to the ingestion of turbulence by a subsonic rotor:

$$\frac{\langle S_1\rangle}{\rho_0 a_0^3\Omega^{-1}M_t^2(R_T/r)^2}=\frac{16\pi^4B^2M_0^4}{1-M_0^2}\left(\frac{bc}{R_T^2}\right)^2\left(\frac{R_T}{R_0}\right)^2\left(\frac{\Omega\Lambda}{V_c}\right)^3\left(\frac{f}{\Omega}\right)^2 \cdot\int_{-\infty}^{\infty}d\xi\,\xi\sum_{n=n_1}^{n_2}\sum_{l=-\infty}^{\infty}E_{mn}E_lE_{turb}\left(E_{chord}E_{span}\right) \tag{3}$$

where the introduced factors are defined by the following.

$$\xi_{mn}=\left|\frac{\frac{f}{\Omega}-\overline{nB}}{(V_c/\Lambda\Omega)}\right|,\quad n_{1,2}=\left[\frac{\frac{f}{\Omega}\mp\left(\frac{V_c}{\Lambda\Omega}\right)\xi}{B}\right]$$

$$E_{mn}=\left[\cos\mu\sin\phi-\frac{(nB-l)\sin\mu}{M_0(F/\Omega)}\right]^2J_{nB-l}^2\left(M_0\frac{f}{\Omega}\cos\phi\right) \tag{3.1}$$

$$E_l=J_l^2\left(\frac{M_0}{M_c}\sqrt{(V_c/\Lambda\Omega)^2\xi^2-\left(\frac{f}{\Omega}-nB\right)^2}\right) \tag{3.2}$$

$$E_{turb}=\frac{\left(\frac{V_c}{\Lambda\Omega}\right)^2\xi^2-\left(\frac{f}{\Omega}-nB\right)^2}{\left(1+4\pi^2\xi^2\right)^3} \tag{3.3}$$

$M_0$, $M_c$, and $M_t$ are the rotational, convective, and r. m.s. turbulence Mach numbers, respectively. $\xi = \nu\Lambda$ is the dimensionless turbulence wave number magnitude; $R_T$ and $R_0$ represent the tip radius and effective radius of rotation of the point dipoles, respectively. The notation $\overline{nB}$ denotes the blade passing frequency nearest to $f/\Omega$. The theoretical model developed by Homicz is a general exact formulation, for which expressions for the turbulence spectrum and the unsteady aerodynamic transfer function($E_{aero}$) are available. For this study, the transfer functions for unsteady aerodynamics and spanwise distributed loading effects provided by Homicz is used as the order of magnitude corrections at high frequencies.

## Ⅳ. Computational Results

### 4.1 Monopole consideration

Fig. 1 and 2 illustrates the comparison of present calculation and experimental data[8] of $1/7^{th}$ scale UH-1H helicopter rotor in nonlifting hover. The UH-1H rotor utilizes the NACA 0012 airfoil with an aspect ratio of 13.71 and is composed of two rectangular blades. The observer is located in the plane of rotation where the monopole noise

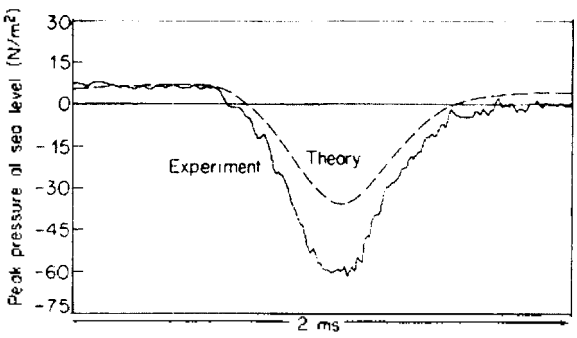


(a) Experimental and linear theory

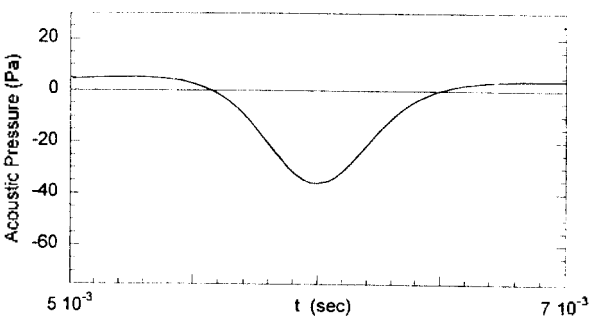


(b) Present calculation

Figure 1. Comparison of the current prediction with the experimental pressure time history, in plane, $r = 3r_T$, $M_T = 0.8$

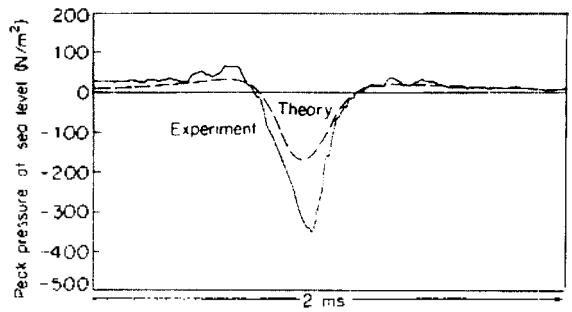


(a) Experimental and linear theory

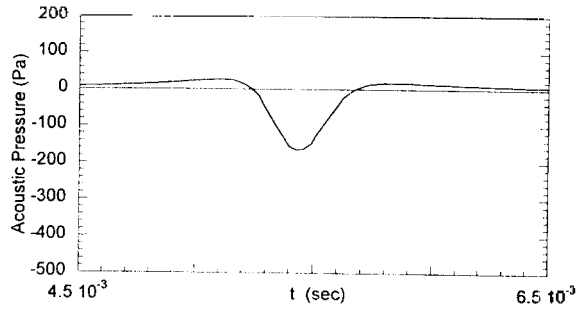


(b) Present calculation

Figure 2. Comparison of the current prediction with the experimental pressure time history, in plane, $r = 3r_T$, $M_T = 0.88$

is maximum. The experimental data is provided with the theoretical result which shows good agreement with current calculation both in the wave form and the magnitude of the negative pressure peak. The discrepancy between the prediction with experiment in the magnitude of the pressure peak results from the crude modeling including only the monopole term in the FWH equation. The disagreement is greater with increased tip Mach number where the nonlinear flow phenomena such as shock and turbulence related mechanisms contribute to the generation of noise.

### 4.2 Dipole consideration

To investigate the dipole characteristics of a rotor in hover, dipole calculation based on the pressure data obtained by the theory of thin wing sections[9] is carried out. A lifting hover condition with collective pitch of 8° is imposed on a rectangular blade with an aspect ratio of 6. The two bladed rotor is operated at a tip Mach number of 0.44 and the induced angle of attack of 3.8° is used. The thin wing section theory yielded a surface pressure data reasonably in accordance with the experimental data provided by F. X. Caradonna and C. Tung[10]. The calculated wave form and spectra are shown in fig. 3 and

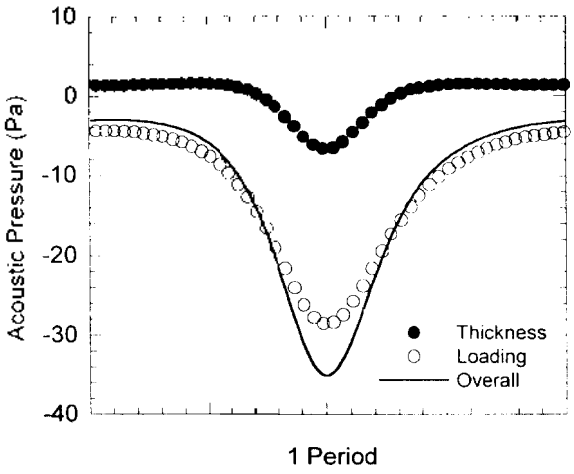


Figure 3. Acoustic pressure signatures of the noise components, $\phi = 20°$, $r = 1.5r_T$

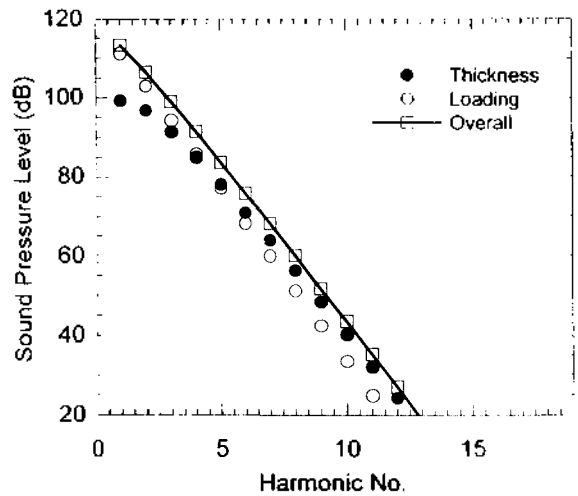


Figure 4. Acoustic spectra of the noise components, $\phi = 20°$, $r = 1.5r_T$

Fig. 4, respectively. Here the dipole term is shown to dominate the first few harmonics, which contribute greatly to the overall noise level.

### 4.3 Turbulence ingestion noise

Fig. 5(a) shows the calculated noise spectra using eqn. 2 and eqn. 3. The model used here is a four bladed rectangular rotor with a NACA 0012 airfoil section throughout. The operating condition is a simulated vertical ascent with a controlled turbulence generating grid upstream as experimented by Paterson and Amiet.[11] The calculated results show steady loading noise dominating the first few harmonics with turbulence ingestion noise demonstrating its broadband characteristics. The steady loading generates the maximum level of noise at the first BPF, 263.

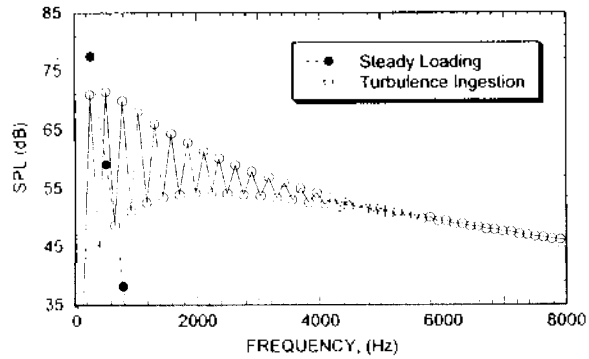


(a) Numerical Predictions

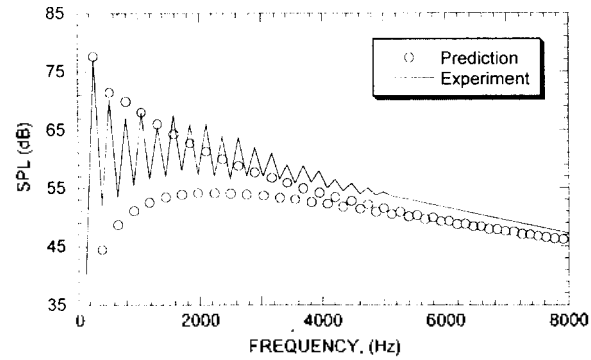


(b) Total Prediction vs. Experimental Data

Figure 5. Noise spectra of the rotor ingesting turbulent flow, high turbulence level, $(\overline{w^2})^{1/2} = 1.3m/s$, $\phi = 30°$, $M_T = 0.47$

2Hz, decaying rapidly with the frequency. The examination of the result revealed that the steady loading noise is dominated by the monopole thickness contribution.

Fig. 5(b) illustrates the calculated result with experimental data. The peaks in the experimented spectrum is centered at the rotor's BPFs, but shows the tone broadening typical of turbulence ingestion phenomenon. The agreements between the experiment and calculation at the first two BPFs are excellent. This speculation is important in two ways. From a practical point of view, the prediction of the overall noise level, following the accurate prediction of the noise levels from the dominant frequencies, is achieved. Since the overall noise level is of primary concern in most applications, this result establishes the usefulness of the current method in practical applications. While the trends in the higher frequency region are simulated by the turbulence ingestion broadband analysis, the agreements at the low frequency are greatly enhanced by the combined consideration of steady loading contributions. This 'combination technique' also enables the user to distinguish the noise generation mechanisms that contribute to a given noise spectrum.

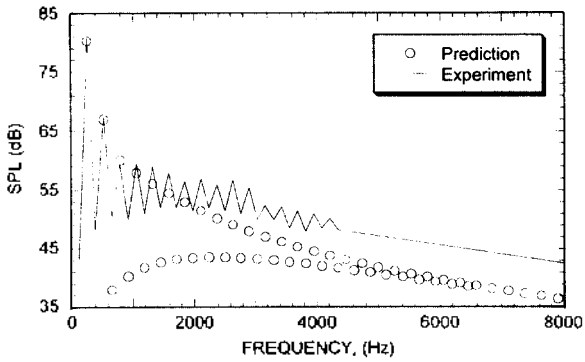


Figure 6. Noise spectra of the rotor ingesting turbulent flow, high turbulence level, $(\overline{w^2})^{1/2} = 1.3m/s$, $\phi = 10°$, $M_T = 0.47$

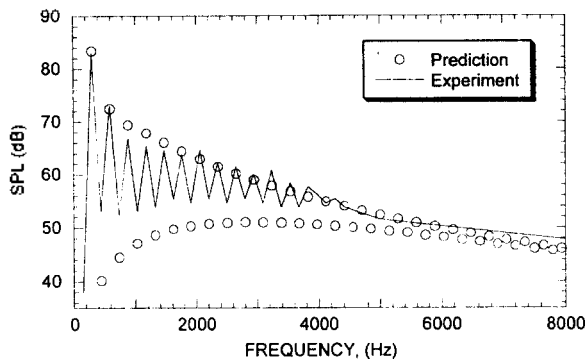


Figure 7. Noise spectra of the rotor ingesting turbulent flow, moderate turbulence level, $(\overline{w^2})^{1/2} = 0.8m/s$, $\phi = 30°$, $M_T = 0.52$

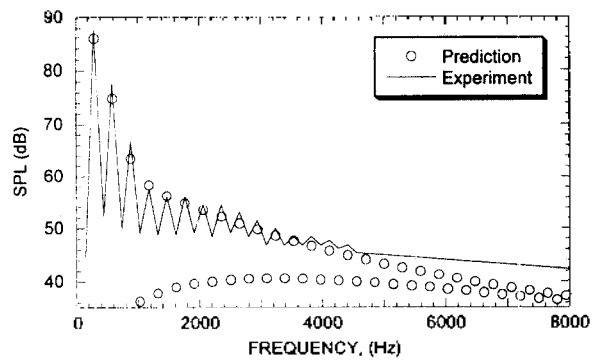


Figure 8. Noise spectra of the rotor ingesting turbulent flow, moderate turbulence level, $(\overline{w^2})^{1/2} = 0.8m/s$, $\phi = 10°$, $M_T = 0.52$

Fig. 6 shows the noise spectra of the same test condition with changes in the observer position. The increase in the level of the first BPF noise near the rotor plane confirms the monopole source contribution. The broadband noise level in the high frequency range is not as well predicted as in the previous position, the predicted level falling below that of experiment. Fig. 7 and Fig. 8 each corresponds to the observer positions for Fig. 5 and Fig. 6, respectively, but with different test conditions. The increased level of noise in the first few BPFs result from the higher rotational speed. The agreement between predicted noise spectra and experimental spectra is similar to that discussed in the case of higher turbulence level; that is, the trends in the higher frequency region are well simulated by the turbulence ingestion broadband analysis, while the agreements at the low frequency are achieved by the steady loading contributions. Of note is the similar tendency of the high frequency broadband underprediction near the plane of rotation. Although the lack of experimental data and the extensive amount of calculation time required for the evaluation of high order Bessel functions in equation (3) limit the comparison to 8000Hz, the discrepancy of the broadband noise level near the rotor plane manifests the existence of a different broadband noise mechanism with strong radiation characteristics near the plane of rotation.

## V. Summary and Conclusions

Numerical predictions of aerodynamic noise radiated by subsonic rotors have been carried out. Both discrete frequency noise as well as broadband noise arising from the ingestion of turbulence have been considered. Using Farassat's 1A formulation of time domain acoustic analogy approach, the monopole noise wave forms of a model helicopter rotor have been predicted. The agreement with linear theory is good and the wave form is correctly predicted in comparison to the experiment. Dipole noise from a rotor in lifting hover has been calculated through the blade loading obtained by the theory of thin wing sections. The successful noise prediction using a simple modeling for blade loading demonstrated the capability of the current method in predicting rotor noise without extensive calculation of the blade loading. Broadband noise from turbulence ingestion has been combined with the discrete frequency noise to predict the overall noise spectrum. The comparison with the experimental results showed excellent agreements for the first few BPF noise levels followed by a reasonable correspondence in the mid-to-high frequency region. Calculation from various observer positions revealed the existence of a different broadband noise mechanism with strong radiation tendency to the rotor plane. It is seen that the contributions from different noise mechanisms can also be analyzed through this method.

## References


1. Hawkings, D. L. and Lowson, M. V., "Theory of Open Supersonic Rotor Noise," *Journal of Sound and Vibration*, Vol. 36, 1974, pp. 1-20.
2. Coffen, C. D., Tillman, G., and Davis R. L., "Transferring Aerospace Technology to Commercial Products: Aeroacoustic Prediction Methods for Automobile Radiator Fans," FED-Vol. 219, *Computational Aeroacoustics, ASME*, 1995.
3. Ffowcs Williams, J. E. and Hawkings, D. L., "Sound Generated by Turbulence and Surfaces in Arbitrary Motion," *Philosophical Transactions of the Royal Society*, A264, 1969, pp. 321-342.
4. Lighthill, M. J., "On Sound Generated Aerodynamically, I. General Theory," *Proc. Roy. Soc.* A, Vol. 211, 1952, pp. 564-587.
5. Paul A. Nystrom and F. Farassat, "A Numerical Technique for Calculation of the Noise of High-Speed Propellers with Advanced Blade Geometry," *NASA TP 1662*, 1980.
6. Farassat, F. and Succi, G. P., "The Prediction of Helicopter Rotor Discrete Frequency Noise," *Vertica*, vol. 7, no. 4, 1983, pp. 309-320.
7. Homicz, G. F. and George, A. R., "Broadband and Discrete Frequency Radiation from Subsonic Rotors," *Journal of Sound and Vibration*, vol. 36, 1974, pp. 151-177.
8. Schmitz, F. H. and Yu, Y. H., "Helicopter Impulsive Noise: Theoretical and Experimental Status," *Journal of Sound and Vibration*, vol. 109, pp. 361-422, 1986.
9. Abbott, Ira H. and Von Doenhoff, Albert E., *Theory of Wing Sections*, Ddver Publ., Inc., c. 1959.
10. Caradonna, F. X. and C. Tung, "Experimental and Analytical Studies of a Model Helicopter Rotor in Hover," *NASA TM 81232*, 1980.
11. Paterson, R. W. and Amiet, R. K., "Noise of a Model Helicopter Rotor Due to Ingestion of Turbulence," *NASA CR 3213*, 1979.



▲Jeonghan Lee

Jeonghan Lee received his B.S. and M.S. degrees in Aerospace Engineering from Seoul National University, Seoul, Korea, in 1995 and 1997, respectively. He has been working with the Institute of Advanced Machinery and Design since 1995. His current interests include aerodynamics and aeroacoustics of commercial fans, helicopter rotors, and propellers.

▲Soogab Lee

Soogab Lee received his B.S. and M.S. degrees in Aerospace Engineering from Seoul National University, Seoul, Korea, in 1983 and 1985, respectively. He received his Ph.D. degree from Stanford University in 1992 and joined NASA Ames Research Center. He is a senior member of American Institute of Aeronautics and Astronautics(AIAA) and a member of many international/domestic institutes. He is currently a professor of Aerospace Engineering at Seoul National University with research interests in various fields of acoustics ranging from aeroacoustics to active noise control.